Thermal quench induced heat fluxes on ASDEX Upgrade

Raphael Schramm[1], T. Eich[2], M. Faitsch[1], M. Maraschek[1], R. McDermott[1], R. Sweeney[2], H. Zohm[1], the ASDEX Upgrade Team[†], and JET contributors[‡]

[1]*Max-Planck-Institut für Plasmaphysik, Garching b. München, Germany*
[2]*Commonwealth Fusion Systems, Devens, MA, USA*
[†]*See the author list of H. Zohm et al, Nucl. Fusion 64 (2024) 112001*
[‡]*See the author list of C.F. Maggi et al, Nucl. Fusion 64 (2024) 112012*

Introduction

Unmitigated disruptions pose a risk for tokamak operation, especially the larger machines currently in the planning or building phase. Therefore, they must be avoided or sufficiently mitigated. While some aspects have been studied extensively, the divertor heat fluxes have received less attention. During the thermal quench (TQ), most of the plasma thermal energy is lost via radiation or conducted to the divertor.

Empirical scalings put the resulting heat flux at least one order of magnitude above the tungsten melt limit for devices such as ITER or SPARC. Previous work has established estimations for the TQ duration, the energy fraction conducted to the divertor, and the area subjected to the peak heat flux [1]. However, extrapolation to future devices requires a multi-machine scaling, which is incomplete. In particular, the deposition time in the divertor, which is different from the core collapse time, needs further investigation.

ASDEX Upgrade (AUG) features an infrared diagnostic system, that measures the divertor temperature and has been operating, with some changes, for the last three decades. With this system the relevant TQ parameters can be determined. While most disruptions are mitigated, a sufficient amount of unmitigated cases is available.

The AUG IR system and data output

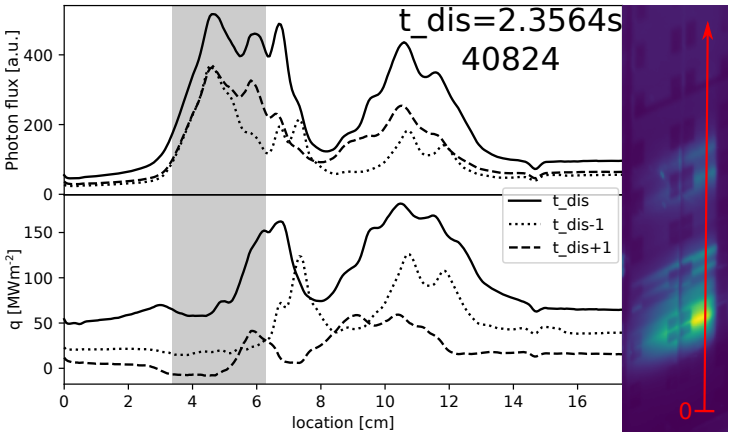

Figure 1: Frame from the AUG IR camera (right) during a TQ and the corresponding intensity and heat flux profiles

For this work, the infrared camera looking at the lower, outer divertor target of AUG is used [2]. It features a field of view looking at the outer vertical target, where the primary strike point is usually located. An example of a frame recorded by this camera during a TQ can be seen in figure 1. The measured intensity is proportional to the surface temperature of the tile. A line, parallel to the tile edge, is then set through the intensity maximum in the field of view. Along this line, the heat flux is calculated using the THEODOR [3, 2, 4] code.

Figure 1 shows also the intensity measured by the camera and the resulting heat flux during a TQ and the previous and next frames. In contrast to what is observed for ELMs, the structure features multiple spatially separated heat flux peaks of comparable height. Further, the background heat flux is considerably above zero. Finally, the peak heat flux does not occur at the position, where the primary strike line was previously located (area marked in gray).

From this heat flux profile a "wetted area" ($A_{wet} = 2\pi R q_{max}^{-1} \int dx\, q(x)$) describing the area affected by the heat flux (q) can be calculated [5]. Note that this definition is typically used for ELMs, where the background is much smaller.

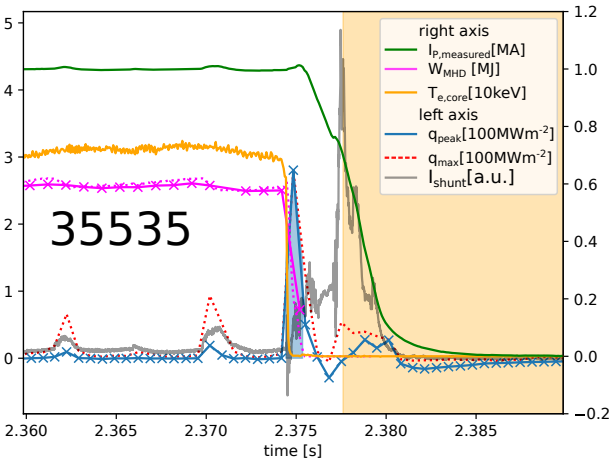

Figure 2: Time evolution of IR heat flux

In order to get information regarding both the TQ duration (τ) and the deposited energy fluence ($\varepsilon_\perp$), the time evolution must be considered. Figure 2 shows the time evolution of the heat flux at the position of the maximum during the TQ in blue, with the overall maximum shown in red. Between data points, a linear interpolation is used. The TQ is clearly visible. For comparison, I_p, W_{MHD}, core T_e and divertor shunt current measurements are also shown. From this data, τ is defined as the 1/e width of the TQ peak. Note that as the IR time resolution is rather poor, the uncertainty on this measurement is large. For $\varepsilon_\perp$, the integral over the TQ peak is used. With a similar setup, data is available from carbon-AUG [3] and from JET [6].

Results from the dataset

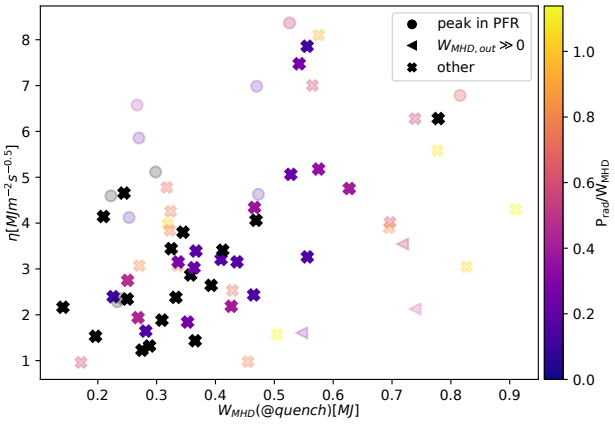

Figure 3: Energy impact against W_{MHD}; "Outliers" and high f_{rad} cases shown with reduced opacity

The current version of the AUG IR system has been operating for $\sim$ 10000 discharges. For this work, only cases with an unmitigated TQ of sufficient power (arbitrarily limited to $W_{MHD} \gtrsim 0.2$ MJ) are considered. The resulting dataset consists of $\sim$ 70 discharges. Note that a lot of discharges are "lost" to the database, due to successful mitigation action. The measured heat impact ($\eta = \varepsilon_\perp \tau^{-0.5}$) as function of stored energy (W_{MHD}) is shown in figure 3. If all data points are considered, the scatter is rather large.

There are two noteworthy configurations that will be called "outliers" for the rest of this work: Cases with $W_{MHD} \gg 0$ after the TQ, showing a lower heat impact are marked with a triangle (as the equilibrium reconstruction does not work reliably post TQ, a consistent ΔW_{MHD} is not

available) and cases where the peak heat flux occurs in the previously private flux region are marked with a circle. Additionally, the radiation can be considered. To separate TQ radiation from current quench radiation, the standard time resolution of the AUG foil bolometers is insufficient. An evaluation with reduced integration time, and thereby better time resolution, is used instead at the cost of increased uncertainty ($\sim 30\%$) and some cases where the evaluation fails (marked in black). If both the "outliers" and cases with a radiation fraction above 50 % are ignored, the ordering provided by the stored energy improves considerably.

Similar to the "Eich-scaling" for ELMs [8], a rather strong correlation is seen between η and the pedestal top pressure. When investigating this, it was found, that a large fraction of disruptions considered here have an intact pedestal prior to the disruption, which is unexpected and may indicate a bias of the dataset.

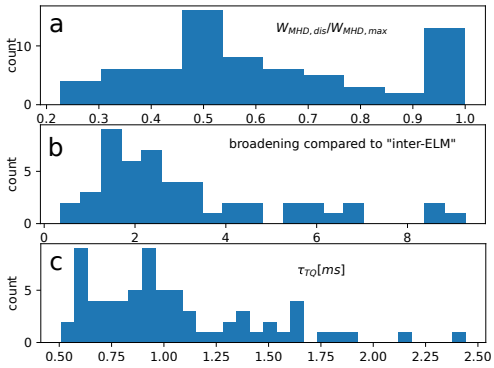

Figure 4: Distributions of relative disruption energy, strike point broadening and TQ duration

Figure 4a shows the stored energy at the time of the disruption compared to the maximum during a discharge. While the majority of cases do show a pre-TQ energy loss, the maximum is at a higher value than shown in [1], and the peak close to the full energy is much higher. Figure 4b shows the strike point broadening, calculated by dividing the TQ wetted area by an inter-ELM value. Notably, most cases are in the 1.5-3.5 range, which is considerably below the broadening factor of 7 stated in [1]. Figure 4c shows a distribution of the thermal quench duration based on IR measurements. The large peak on the left is likely an artifact of the camera time resolution. Notably all of these are considerably above the IPB scaling law [7], which would expect $\sim$0.2 ms for AUG. They are also significantly larger than the core collapse time seen by the ECE (shown in figure 2) or soft x-ray systems, indicating that these two parameters are likely not equal as it has been sometimes assumed.

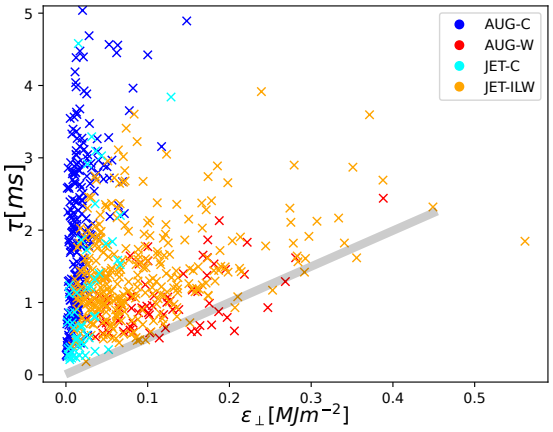

Figure 5: TQ duration against energy fluence; a separation of C and W cases and an indicated lower bound can clearly be seen

An interesting result becomes visible when comparing τ and $\varepsilon_\perp$. Figure 5 compares AUG-W data to AUG-C data, and an arbitrary selection of JET cases. Both a lower bound and a separation of C and W cases are clearly visible. Numbers are not given, as an uncertainty quantification is not yet available. The behavior would be consistent with the W cases being sheath limited, and the C cases radiation limited. This could explain the discrepancy of the TQ duration to the IPB scaling law, which includes mostly carbon machines.

Comparison to a simple scaling

Figure 6 shows a comparison between a simplistic energy balance, assuming that all of the lost energy is conducted to the divertor, and the measured value of η. It can be seen that the energy impact is overestimated. This is, despite using a power sharing factor of 0.5 between inner and outer target in the model. Typically, significantly more power reaches the outer target, which would make the points move right in the figure. While details are still challenging due to the large uncertainties, e.g. on the radiated fraction, the threat seems to be smaller than assumed by such a scaling.

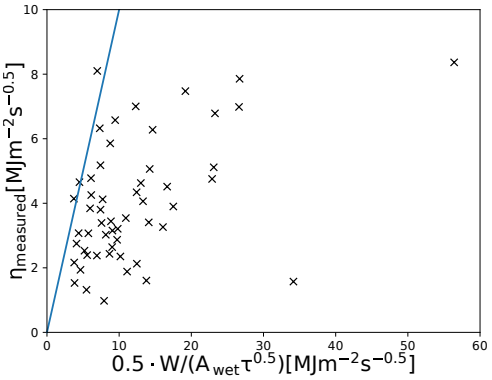

Figure 6: Measured η against scaling, including a 1:1 line

Summary and outlook

A study has been carried out looking at TQ heat fluxes on AUG. The data shows discrepancies from previously used assumptions [1, 7], notably a longer TQ duration and a smaller strike point broadening. Thermal quenches seem to be happening at a higher energy fraction than seen on JET. At the same time the AUG dataset has a high fraction of cases with intact pedestal at the time of disruption, which is not observed in other machines. This may indicate a bias in the dataset towards a higher power disruption where the mitigation system may be less reliable. Looking at the dependency of τ against $\varepsilon_\perp$, a clear lower bound is seen. This would be consistent with sheath limited heat flux for a W wall, which could explain the longer than expected TQ duration. Comparison to an energy balance shows a more benign behavior in experiments than assumed from the scaling. Finding the remaining loss channels is of interest for future work.

Acknowledgement

This work has been carried out within the framework of the EUROfusion Consortium, partially funded by the European Union via the Euratom Research and Training Programme (Grant Agreement No 101052200 — EUROfusion), and partially funded by Commonwealth Fusion Systems (CFS). Views and opinions expressed are however those of the author(s) only and do not necessarily reflect those of the European Union, the European Commission or CFS. Neither the European Union nor the European Commission nor CFS can be held responsible for them.

References

[1] Hender et al, Nuclear Fusion **47** S128, 2007
[2] Sieglin et al, Rev. Sci. Instrum. **86** 113502, 2015
[3] Herrmann et al, Plasma Phys. Control. Fusion **37** 17, 1995
[4] Nille et al, Springer Proceedings in Mathematics & Statistics, **239** 55, 2017
[5] Eich et al, Journal of Nuclear Materials **415** S856, 2011
[6] Balboa et al, Plasma Phys. Control. Fusion **65** 094002, 2023
[7] ITER Physics Basis, Nuclear Fusion **39** 2251, 1999
[8] Eich et al, Nuclear Materials and Energy, **12** 84, 2017